NEW PARAMETRIZATION FOR OPTICAL MODEL DESCRIPTION OF ELASTIC α-PARTICLE SCATTERING FROM HEAVY NUCLEI OVER A WIDE ENERGY RANGE*

By Z. Majka and T. Srokowski

Institute of Physics, Jagellonian University, Cracow**

(Received June 16, 1977)

Differential cross sections for elastic scattering of α-particles from ^{90}Zr, ^{92}Zr, ^{124}Sn and ^{208}Pb were analysed over available energy range in terms of the optical model. New parametrization of the energy dependence of the optical potential parameters was used. Satisfactory agreement of the model predictions and experimental data was obtained.

1. Introduction

In the recent years, with increasing availability of accelerator facilities a considerable amount of the experimental data for scattering of α-particles from nuclei has been accumulated. In order to be able to apply the analysis by the method of distorted waves, coupled channels and the like, it is necessary to treat the elastic scattering channel adequately. Most of the data for elastic α-particle scattering have been analysed in terms of the optical model in which the projectile-target nucleus interaction is represented by a complex potential. The real part of this potential usually has a phenomenological form or is calculated in microscopic way [1, 2]. For the imaginary potential the phenomenological Woods-Saxon (W–S) potential has usually been used.

Although early analyses provided good description of the experimental data for some nuclei and limited energy regions, the energy dependence of the optical model parameters was poorly determined and frequently non physical. Moreover, the potential parameters had discrete and continuous ambiguities.

The aim of this paper is to determine the alpha particle-nucleus phenomenological potential for heavy target nuclei by simultaneously analysing all the angular distributions

* Supported by the National Science Foundation through the Maria Skłodowska-Curie Found, contract No 01316.

** Address: Instytut Fizyki UJ, Reymonta 4, 30-059 Kraków, Poland.

of the elastic scattering in the available energy range. The phenomenological representation of the form-factor of the potential was found in the microscopic way in our preceding paper [2].

2. *Optical model analysis of the data*

Data on the elastic scattering of α-particles from ^{90}Zr and ^{92}Zr were chosen for the analysis, since for these nuclei the most extensive measurements are available. Moreover, data on the elastic scattering of α-particles from ^{124}Sn and ^{208}Pb were chosen, because the available energy range and sufficiently large angular range allow one to resolve the discrete ambiguities of the depth of the potential [3]. The energies and the references of the angular distributions analysed are given in Table II.

The calculations were carried out using the alpha-target interaction in the form

$$V(r) = V_c(r) - Uf(r, D_1, d_1) - i\left[W_v f(r, D_2, d_2) - 4d_3 W_s \frac{d}{dr} f(r, D_3, d_3)\right], \tag{1}$$

where $V_c(r)$ is the Coulomb potential due to a uniformly charged sphere with a radius $R_c = 1.34\,A^{-1/3}$ and

$$f(r, D_i, d_i) = \left[1 + \exp\left(\frac{r - D_i}{d_i}\right)\right]^{-2}. \tag{2}$$

The present form of the form-factor argued in our preceding paper [2], results from microscopic calculations. The usually used volume imaginary potential was supplemented by the surface term. This form of the imaginary potential was necessary to fit the ^{58,60}Ni(α, α) data in the large energy range of scattering [4] and was accepted by analogy with nucleon-nucleus calculations (see [5] and references quoted therein).

The energy dependence of the optical potential has been parametrized in the following way [4]

$$U = A_1 + A_2 E_\alpha, \tag{3}$$

$$W_v = A_3 + A_4 \exp(-A_5 E_\alpha), \tag{4}$$

$$W_s = A_6 + A_7 \exp(-A_8 E_\alpha), \tag{5}$$

where E_α is the energy of the alpha projectiles. The parameters of the form-factors were energy independent.

In the optical model analysis the GLOB code [6] was used. An automatic search routine varied parameters in order to minimize simultaneously the value of χ^2 for all of the angular distributions. The best fit parameters are contained in Table I. Figure 1 presents comparison of the model predictions with the experimental data. Table II contains values of χ^2 per point.

TABLE I

Optical model global best fit parameters

Parameters	$^{90}Zr(\alpha, \alpha)$	$^{92}Zr(\alpha, \alpha)$	$^{124}Sn(\alpha, \alpha)$	$^{208}Pb(\alpha, \alpha)$
A_1 [MeV]	177.17	177.07	178.82	195.05
A_2	−0.2189	−0.2610	−0.2038	−0.2094
$D_1A^{-1/3}$ [fm]	1.3854	1.3794	1.3342	1.3893
d_1 [fm]	1.2259	1.2114	1.2589	0.933
A_3 [MeV]	20.49	20.71	27.61	26.19
A_4 [MeV]	−30.36	−29.47	−39.83	−41.46
A_5 [MeV^{-1}]	0.0222	0.0248	0.0339	0.0301
$D_2A^{-1/3}$ [fm]	1.7333	1.7235	1.5784	1.5686
d_2 [fm]	1.0009	1.2209	1.3932	1.6238
A_6 [MeV]	0.7237	2.9953	3.2610	6.4187
A_7 [MeV]	47.37	54.90	60.00	90.95
A_8 [MeV^{-1}]	0.0184	0.0205	0.05	0.902
$D_3A^{-1/3}$ [fm]	1.3261	1.3283	1.3450	1.3364
d_3 [fm]	0.4068	0.4291	0.4472	0.4410

TABLE II

Values of the χ^2 per point

E_α [MeV]	$^{90}Zr(\alpha, \alpha)$		$^{92}Zr(\alpha, \alpha)$		$^{124}Sn(\alpha, \alpha)$		$^{208}Pb(\alpha, \alpha)$	
	χ^2/N	Ref.*	χ^2/N	Ref.*	χ^2/N	Ref.*	χ^2/N	Ref.*
26.2	106.1	14						
40	16.1	10	12.8	10				
59.1	69.4	10						
79.5	13.4	10						
90			21.7	10				
99.5	9.8	10						
104					6.5	11	18.3	11
118	13.2	10						
120			13.1	10				
139							26.6	13
166	30.1	12			29.8	12	46.2	12

* References to the experimental data.

3. *Discussion*

As can be seen in Fig. 1 an essentially good description of the experimental data was achieved in whole energy range with the parametrization of the optical potential as given in the preceding section. The global best fit parameters (see Table I) are similar for different target nuclei.

The depth of the real part of the potential decreases linearly with the increase of the energy of the alpha-particles (Fig. 2) with the slope of about −0.2 MeV/MeV. This value

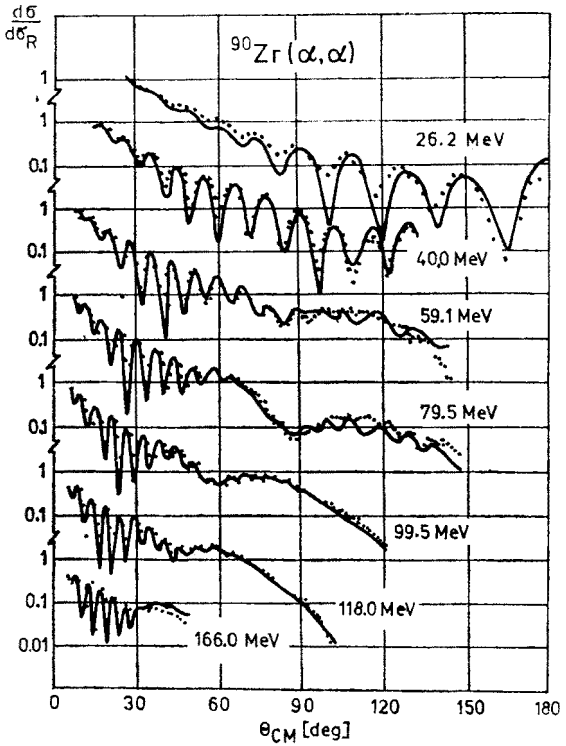

Fig. 1a. Comparison of the experimental angular distributions for the $^{90}Zr(\alpha, \alpha)$ scattering (dots) with those calculated with the optimum parameter set given in Table I (solid line)

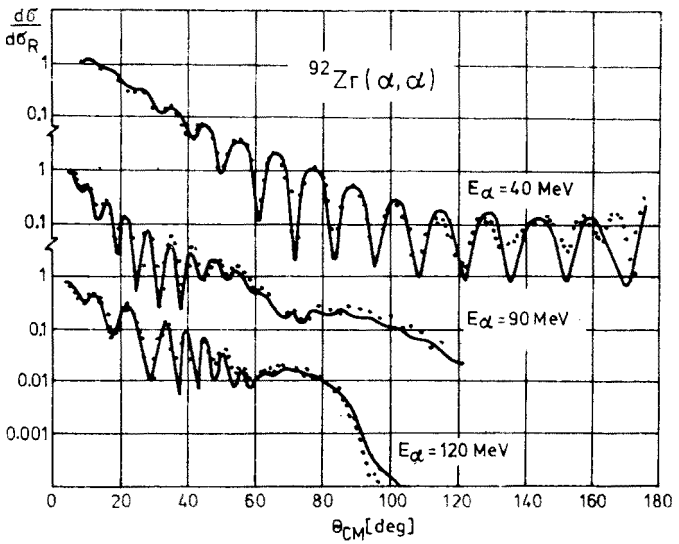

Fig. 1b. The same as in Fig. 1a but for the $^{92}Zr(\alpha, \alpha)$

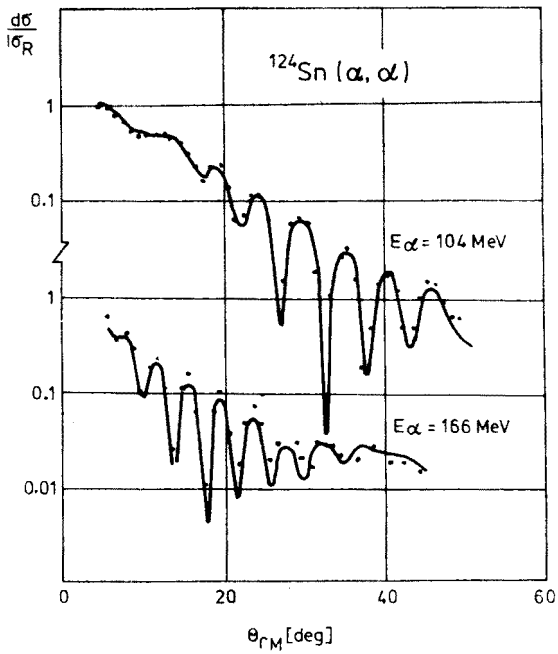

Fig. 1c. The same as in Fig. 1a but for the $^{124}Sn(\alpha, \alpha)$

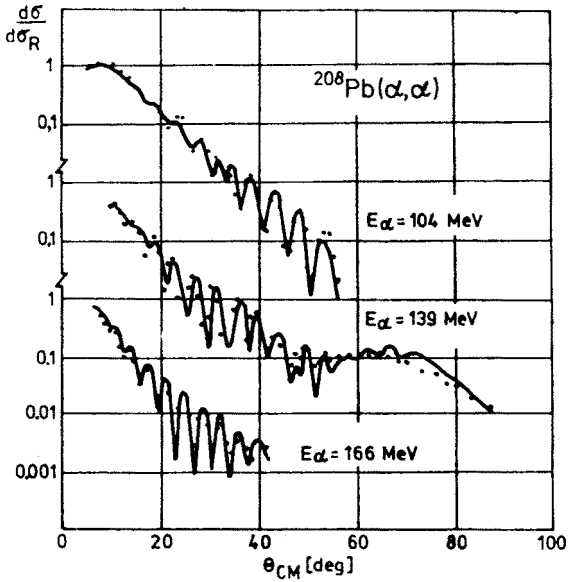

Fig. 1d. The same as in Fig. 1a but for the $^{208}Pb(\alpha, \alpha)$

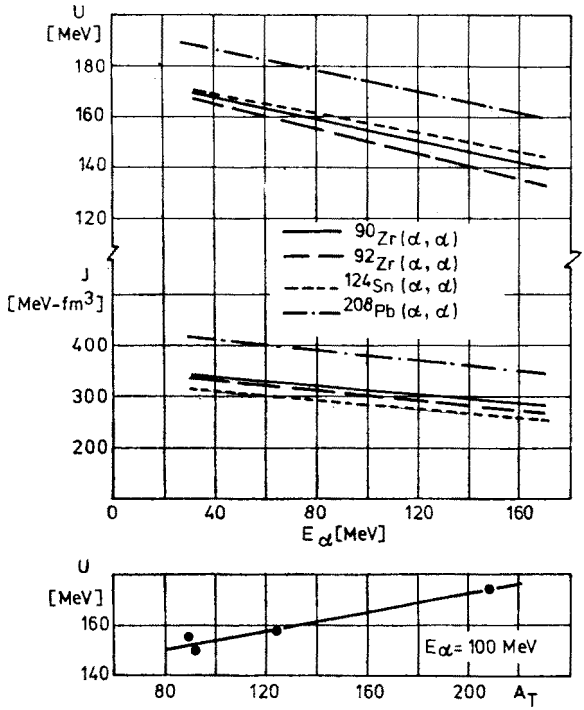

Fig. 2. Energy dependence of the depth of the real potential, U, and of the volume integral per nucleon of the real potential, J, (upper part). Isotope dependence of the depth of the real potential (lower part)

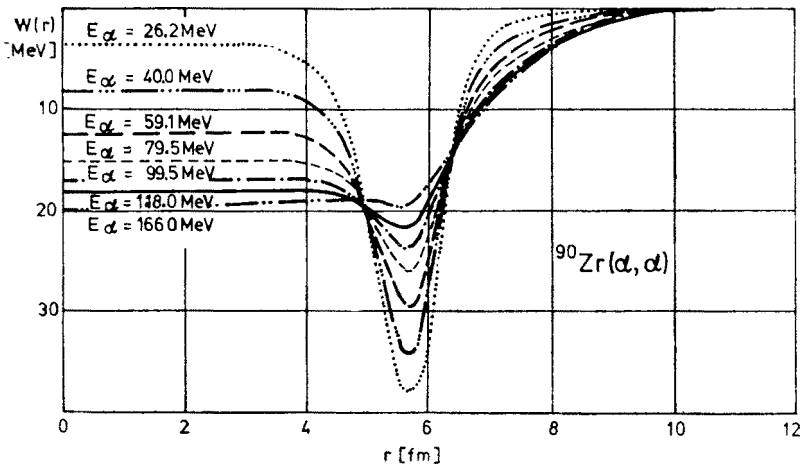

Fig. 3. Energy dependence of the total imaginary potential for the $^{90}Zr(\alpha, \alpha)$ scattering

is in agreement with those found by other authors [7, 8]. Furthermore, the depth of the real part of the potential slightly increases for heavier target nuclei (see Fig. 2). The microscopic calculations performed for alpha-particle [2, 8] and nucleon scattering [9] predicted the above effect. In Fig. 2 the energy dependence of the volume integrals per nucleon is presented. As can be seen the volume integral per nucleon of the real part of the potential varies from 250 MeV fm^3 to 400 MeV fm^3 in agreement with [3, 8, 9].

The energy dependence of the total imaginary potential for the ^{90}Zr(α, α) scattering and the values of the volume integrals for all target nuclei under investigation are given in Figures 4 and 5, respectively. It can be seen that for the lower energies the volume

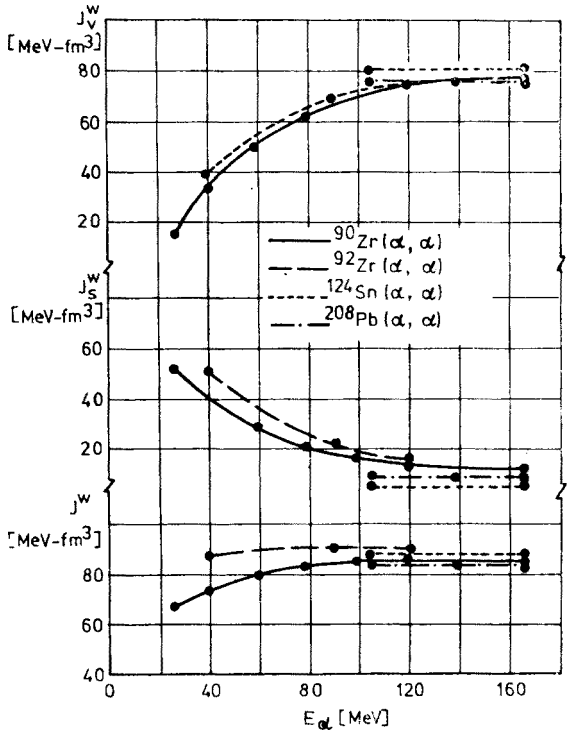

Fig. 4. Energy dependence of the volume integrals per nucleon of the imaginary potential for the volume part, J_v^w, for the surface part, J_s^w, and for the total potential, J^w, respectively. The energies at which the global optical model analysis was performed are indicated by dots

absorption vanishes and the surface absorption takes its place. Moreover, the volume integrals per nucleon of the total imaginary potential are similar for all target nuclei and practically energy independent for higher energies.

The authors would like to express their gratitude to Prof. K. Grotowski for guidance and critical reading of this paper and to Prof. A. Budzanowski and Prof. A. Strzałkowski for helpful discussions. The authors are deeply indebted to Professor G. W. Greenlees, Drs L. W. Put, L. Brissaud and B. Tatischeff for kindly sending numerical data prior to publication.

REFERENCES

[1] A. Budzanowski, A. Dudek, K. Grotowski, Z. Majka, A. Strzałkowski, *Part. Nucl.* **5**, 97 (1973) and references quoted therein.

[2] Z. Majka, A. Budzanowski, K. Grotowski, A. Strzałkowski, Raport INP No 940/PL, Cracow 1977.

[3] D. A. Goldberg, S. M. Smith, *Phys. Rev. Lett.* **29**, 500 (1972); D. A. Goldberg, S. M. Smith, H. G. Push, P. G. Roos, N. S. Wall, *Phys. Rev.* **C7**, 1938 (1973); D. A. Goldberg, S. M. Smith, G. F. Burdzik, *Phys. Rev.* **C10**, 1362 (1974).

[4] A. Budzanowski et al., Raport INP No 962/PL, Cracow 1977.

[5] C. A. Engelbrecht, H. Fiedeldey, *Ann. Phys.* (N. Y.) **42**, 262 (1967).

[6] H. Dąbrowski, R. Płaneta, Raport INP No 947/PL, Cracow 1976.

[7] G. M. Lerner, J. C. Hiebert, L. L. Rutledge, Jr., A. M. Bernstein, *Phys. Rev.* **6C**, 1254 (1972); P. D. Singh, L. W. Put, C. G. Yang, A. M. J. Paans, Proc. of the Int. Conf. on Nuclear Structure, Volume **1**, Munich 1973, p. 337; D. F. Jackson, R. C. Johnson, preprint, University of Surrey.

[8] P. D. Singh, P. Schwandt, G. C. Yang, *Phys. Lett.* **59B**, 113 (1975).

[9] B. C. Sinha, *Phys. Lett.* **33B**, 279 (1970).

[10] L. W. Put, private communication.

[11] D. Habs et al., Raport Kernforschungszentrum No 18/70–2, Karlsruhe 1970.

[12] L. Brissaud, B. Tatischeff, private communication.

[13] D. A. Goldberg, S. M. Smith, H. G. Pugh, P. G. Roos, N. S. Wall, Technical Raport 73–077, University of Maryland 1973.

[14] G. Greenlees, private communication.